## ANTIBIOTIC RESISTANCE

# Role of AcrAB-TolC multidrug efflux pump in drug-resistance acquisition by plasmid transfer

Sophie Nolivos[1]*, Julien Cayron[1], Annick Dedieu[1], Adeline Page[2], Frederic Delolme[2], Christian Lesterlin[1]†

Drug-resistance dissemination by horizontal gene transfer remains poorly understood at the cellular scale. Using live-cell microscopy, we reveal the dynamics of resistance acquisition by transfer of the *Escherichia coli* fertility factor–conjugation plasmid encoding the tetracycline-efflux pump TetA. The entry of the single-stranded DNA plasmid into the recipient cell is rapidly followed by complementary-strand synthesis, plasmid-gene expression, and production of TetA. In the presence of translation-inhibiting antibiotics, resistance acquisition depends on the AcrAB-TolC multidrug efflux pump, because it reduces tetracycline concentrations in the cell. Protein synthesis can thus persist and TetA expression can be initiated immediately after plasmid acquisition. AcrAB-TolC efflux activity can also preserve resistance acquisition by plasmid transfer in the presence of antibiotics with other modes of action.

The global spread of antibiotic resistance among pathogenic bacteria is one of the biggest concerns in public health and a research priority in microbiology. Dissemination of drug resistance is mainly due to the ability of bacteria to acquire genes through horizontal transfer mechanisms, primarily by bacterial conjugation (*1–3*). During conjugation, DNA is transferred from a donor to a recipient cell by direct contact. The resulting transconjugant cell will, in turn, disseminate the conjugative DNA, generally as a plasmid that carries all the genes required for its maintenance and transfer. Analysis of drug-resistant commensal, environmental, and pathogenic bacteria has revealed a vast array of conjugative plasmids carrying one or multiple resistance genes to most, if not all, classes of antibiotics currently used in clinical treatments (*4*).

Owing to its biological importance, bacterial conjugation has been the focus of extensive study since its discovery by Tatum and Lederberg (*5*, *6*). Genetics and in vitro biochemistry have produced an in-depth description of the molecular basis of conjugation [reviewed in (*7–9*)], whereas genomic approaches have revealed its impact on the spread of drug resistance among bacterial species. However, many aspects of drug resistance spread by conjugation have yet to be described in vivo, including the cellular dynamics of DNA transfer, the timing of expression of the newly acquired genes, the phenotypic conversion of the drug-sensitive recipient into a resistant cell, and the

effect of ambient antibiotics on these processes. To address these questions, we developed an experimental system that enables the real-time visualization of drug resistance transfer by conjugation at the single-cell level.

We investigated the acquisition of tetracycline (Tc) resistance by conjugational transfer of the paradigmatic *Escherichia coli* fertility factor (F) plasmid carrying an insertion of the Tn*10* transposon (F-Tn*10*). The *tet* operon from Tn*10* encodes the TetA efflux pump protein, which exports Tc molecules out of the cell. The TetR repressor, which regulates *tetA* expression in response to the presence of the drug, is also carried on Tn*10*. The transfer of resistance by F-Tn*10* conjugation between a wild-type (WT) F-Tn*10* donor and a WT Tc-sensitive recipient strain is highly efficient. Within 3 hours, we found that 70.3 ± 11.6% of the recipient cells were converted into Tc-resistant transconjugants (Fig. 1A). In the presence of a minimal inhibitory concentration of Tc (10 µg/ml), which inhibits protein translation by targeting 16S ribosomal RNA, we found that 36.2 ± 12.5% of recipient cells still acquired Tc resistance. This unanticipated result indicates that transconjugants were able to produce TetA efflux protein after plasmid acquisition, despite the inhibitory effect of Tc on protein synthesis.

We performed real-time microscopy visualization of F-Tn*10* plasmid transfer from donor to recipient cells and quantified the subsequent production of TetA protein in the resulting transconjugant cells. To do so, we developed an F-Tn*10* plasmid transfer reporter based on the fluorescent *parS*/ParB DNA labeling system (*10*) (Fig. 1B). The *parS* binding site is inserted near the origin of transfer (*oriT*) of the F-Tn*10* plasmid contained in the donor strain, whereas the fluorescently labeled ParB protein is only produced from the plasmid in recipient cells, where

it appears diffusely in the cytoplasm. The F-Tn*10* plasmid is transferred into the recipient cell in single-stranded DNA (ssDNA) form and is converted into double-stranded DNA (dsDNA) by synthesis of the complementary strand. DNA synthesis triggers the recruitment of ParB to the dsDNA *parS* site and forms a fluorescent ParB focus (Fig. 1B and movie S1). The lifetime of the ssDNA plasmid intermediate was estimated by visualizing the essential single-strand-binding protein SSB fused to the yellow fluorescent protein (SSB-YFP) (*11*) in the recipient cells (fig. S1, A to D, and movie S2). Internalization of the ssDNA plasmid leads to the formation of a bright SSB focus in the vicinity of the cell membrane (fig. S1C). These intense SSB foci had a lifetime of ~5 min (fig. S1D) and were replaced by a ParB focus within 5 to 10 min (fig. S1E). Assuming a DNA transfer rate of ~46 kb/min [based on 100 min required for transfer of the 4.6 Mb chromosome of *E. coli* (*12*)], transfer of the ~100 kb F-Tn*10* plasmid should be achieved in ~2 min. Our observations show that internalization of the ssDNA, recircularization, and conversion into the dsDNA form is completed within ~10 min.

To monitor TetA production after plasmid acquisition, we constructed a C-terminal fusion of TetA with the mCherry fluorescent protein (TetA-mCh) expressed from the F-Tn*10* endogenous locus (fig. S2A). TetA-mCh conferred fully functional resistance to tetracycline (fig. S2B) and was homogeneously distributed across the inner cell membrane (fig. S2, C and D, and movies S3 and S4).

These reporter systems enabled the real-time visualization of F-Tn*10* conjugation. Donor cells exhibited membrane TetA-mCh red fluorescence; recipient cells showed diffuse ParB-mNEON green fluorescence; and in transconjugant cells, the formation of a ParB focus was followed by an increase in red membrane fluorescence from TetA-mCh production (Fig. 1B). We performed time-course experiments where snapshots of the conjugating population were acquired every hour after mixing F-Tn*10tetA-mCh* donors and Tc-sensitive recipient cells. The frequency of transconjugants was measured directly at the single-cell level from the number of recipient cells exhibiting ParB foci, and the intracellular red fluorescence was quantified in donor, recipient, and transconjugant subpopulations (Fig. 1C). After 1 hour, about a third of the recipient cell population had received the plasmid, but these cells did not show any increase in fluorescence. Production of TetA-mCh was detected 2 hours after conjugation. Better resolution of the time lag between acquisition of the plasmid and synthesis of TetA-mCh was obtained using time-lapse imaging of conjugation in microfluidic chambers (Fig. 2A and movie S5). Single-cell quantitative analysis showed that TetA-mCh production is detectable 30 min after the appearance of the ParB focus, with variable production rates in the different transconjugant cells (Fig. 2B). Assuming a $t_{50}$ = 22 min maturation time for the mCh protein in *E. coli* (*13*), these results indicate that *tetA-mCh* gene transcription and

[1]Molecular Microbiology and Structural Biochemistry (MMSB), Université Lyon 1, CNRS, INSERM, UMR5086, 69007 Lyon, France. [2]Protein Science Facility, SFR BioSciences, CNRS, UMS3444, INSERM US8, UCBL, ENS de Lyon, 69007 Lyon, France.
*Present address: CNRS - Univ Pau & Pays Adour - E2S UPPA, Institut des sciences analytiques et de physicochimie pour l'environnement et les matériaux (IPREM), UMR5254, 64000 Pau, France.
†Corresponding author. Email: christian.lesterlin@ibcp.fr

mRNA translation into TetA-mCh proteins occur within minutes after the conversion of the F plasmid into dsDNA. Similar expression dynamics were observed for an F-Tn10 plasmid in which the *tetA* gene was replaced by the *mCh* gene (F-Tn10Δ*tetA::mCh*) (fig. S3 and movie S6). To obtain another estimate of the timing of expression of plasmid genes independently of the $P_{tetA}$ promoter, we performed the same analysis using an F-Tn10 $P_{lacIQ1}$*sf*GFP plasmid carrying the *superfolder gfp* gene (*sfgfp*) (14) under the control of the $P_{lacIQ1}$ constitutive promoter (15) (fig. S4, A and B). Production of *sf*GFP, which has a maturation time of $t_{50}$ = 13.9 min (13), was first detected 15 min after ParB focus formation (fig. S4, C and D, and movie S7). These results obtained with different fluorescent reporters show that expression of newly acquired plasmid genes starts within minutes after the conversion of the ssDNA plasmid into the dsDNA form, regardless of their position on the plasmid.

Both time-course and time-lapse analysis reveal that TetA-mCh levels in transconjugant cells surpass basal levels observed in donor cells (Figs. 1C and 2B). This was also observed for mCh production after the acquisition of F-Tn10Δ*tetA::mCh* plasmid (fig. S3D) but not for *sf*GFP produced from the $P_{lacIQ1}$ promoter (fig. S4D). We reasoned that such enhanced expression could be due to the unrepressed activity of the $P_{tetA}$ promoter upon

entry of the plasmid into recipient cells devoid of TetR repressor. This phenomenon, referred to as zygotic induction, was initially proposed by Jacob and Wollman (16) and was supported by a previous report (17). To test this hypothesis, we constructed an F-Tn10*tetA-mCh*Δ*tetR* plasmid by deleting the *tetR* gene and compared TetA-mCh production levels after plasmid transfer into WT TetR-free recipient or into TetR-producing recipient cells (chromosomally encoded, under the control of its natural $P_{tetR}$ promoter or $P_{lacIQ1}$ constitutive promoter) (Fig. 2C). As expected, TetA-mCh production was enhanced in both donor and WT recipient cells devoid of TetR repressor. By contrast, TetA-mCh production was abolished in recipient cells containing preexisting TetR before plasmid entry (Fig. 2C). Zygotic induction, triggered by the absence of TetR repressor in the recipient, boosts *tetA* gene expression and accelerates the conversion of Tc-sensitive recipients into Tc-resistant transconjugant cells capable of Tc efflux, before the parallel production of TetR establishes repression. The observation that TetA production precedes the establishment of repression in the transconjugant cells likely relates to the fact that *tetR* promoter is 10 to 50% the strength of *tetA* promoter (18–20). Consistently, computational simulation of the *tet* operon behavior for cells initially free from TetA or TetR (such as the recipients that have just

acquired the plasmid) predicts an average initial production of 20 to 50 TetA molecules per TetR protein before reaching a steady state (21). At steady state, TetR prevents the excess of TetA that could be lethal for the cell and allows a sensitive detection of the presence of tetracycline as well as a fast regulatory response (22, 23).

Next, we investigated the dynamics of plasmid transfer and TetA production when conjugation was performed in the presence of Tc. We observed that plasmid transfer frequency measured at the single-cell level is unaffected by the presence of the drug (73.1 ± 8.2% in the presence of Tc compared with 74.7 ± 13.4% without Tc after 4 hours) (Fig. 1C). This is consistent with the recent report that antibiotics do not directly regulate the efficiency of horizontal gene transfer per se (24). Time-course experiments revealed that plasmid acquisition is still followed by TetA-mCh production, which is only slightly delayed. These results explain our initial observation (Fig. 1A) by confirming that Tc-sensitive recipients manage to produce TetA despite the translation-inhibitory effect of Tc and are therefore converted into Tc-resistant cells. The ability of recipient cells to synthetize proteins despite the presence of Tc was further confirmed by monitoring the production of *sf*GFP after the acquisition of the F-Tn10 $P_{lacIQ1}$*sf*GFP plasmid (fig. S5A). As observed for TetA-mCh, exposure

**Fig. 1. Live-cell visualization of F-Tn10 plasmid transfer followed by production of TetA efflux pump.** (**A**) Frequency of Tc-resistant transconjugants obtained by F-Tn10 conjugation, estimated by plating assay 3 hours after mixing WT donor and recipient cells (ratio 1:3), in the absence (Ø) and in the presence of Tc (10 μg/ml). Histograms show the mean percentage of recipient cells converted into Tc-resistant transconjugants (T/R+T), with the standard deviation calculated from at least 8 biological repeats (black dots). Donor and recipient colony-forming unit concentrations (CFU/ml) in the conjugation mix are presented in fig. S10A. (**B**) Genetic system allowing microscopy visualization of F-Tn10 transfer and production of TetA. WT F-Tn10*tetA-mCh* donor cells exhibit basal TetA-mCh red fluorescence at the membrane; WT pParB-mNEON recipients exhibit diffuse green fluorescence; transconjugant cells are identified by the formation of a ParB focus followed by an increase in TetA-mCh fluorescence. The strains' phenotypes used for screening and selection assays are indicated in brackets. Indicative microscopy images are shown. Scale bars, 1 μm. (**C**) Violin plots showing the single-cell quantification of intracellular fluorescence (SNR, signal-to-noise ratio) in the population



of cells during F-Tn10*tetA-mCh* conjugation, in the absence and in the presence of Tc. The median, quartile 1, and quartile 3 are indicated by horizontal lines and the mean by a black dot. Black dots above and below the maximum and minimum values correspond to outlier cells. Triangles indicate the presence of data points beyond the axis range. The frequency of transconjugants corresponds to the percentage of recipient cells that exhibit a ParB focus estimated from microscopy images. The number of cells analyzed (*n*) is also indicated.
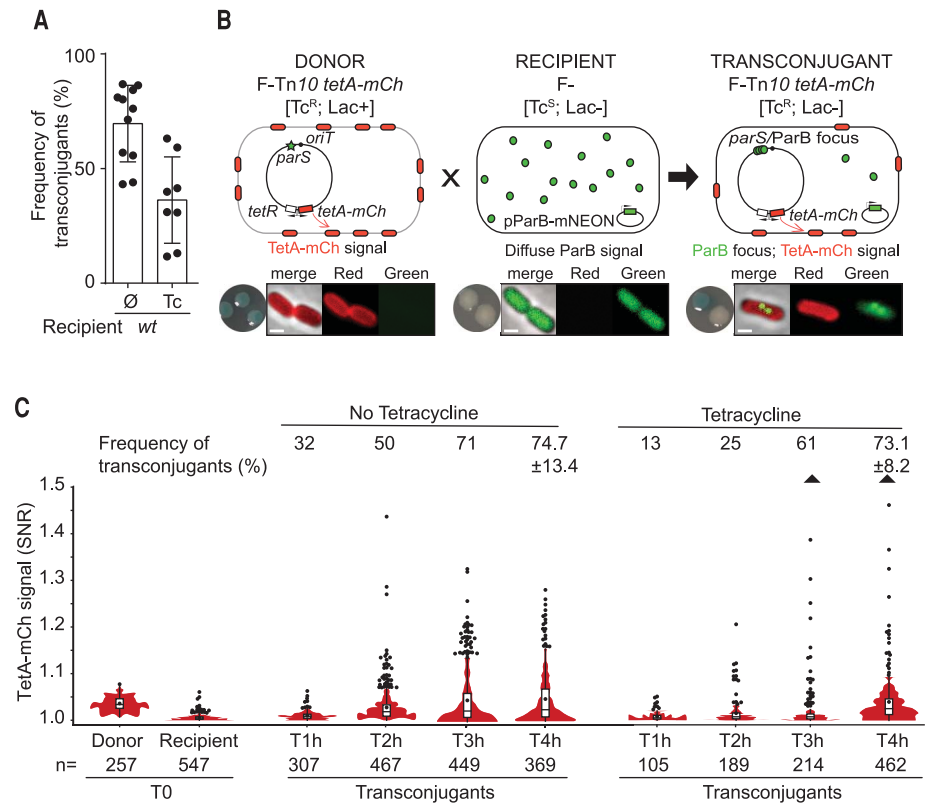
**Fig. 2. Real-time visualization of TetA production after F-Tn10 plasmid transfer and the influence of zygotic induction.**
(**A**) Time-lapse microscopy images of conjugation performed in a microfluidic chamber showing a plasmid-transfer event. Donor (D), recipient (R), and trans-conjugant cells (T) are indicated on the diagram (bottom row). Scale bars, 1 μm. (**B**) Single-cell time-lapse quantification of TetA-mCh signal (SNR) with respect to ParB focus formation in transconjugant cells (0 min). TetA-mCh basal mean signal (SNR) in donor cells is shown by a black dot. Each gray line corresponds to one individual transconjugant, the red line shows the population average with standard deviations (*n* cells analyzed). (**C**) Violin plots showing the single-cell quantification of red fluorescence (SNR) before and after conjugation between WT F-Tn10tetA-mChΔtetR donor and WT, $P_{lacIQ1}$tetR, or $P_{tetR}$tetR recipient strains containing pParB-mNEON plasmid. Same representation as in Fig. 1C.
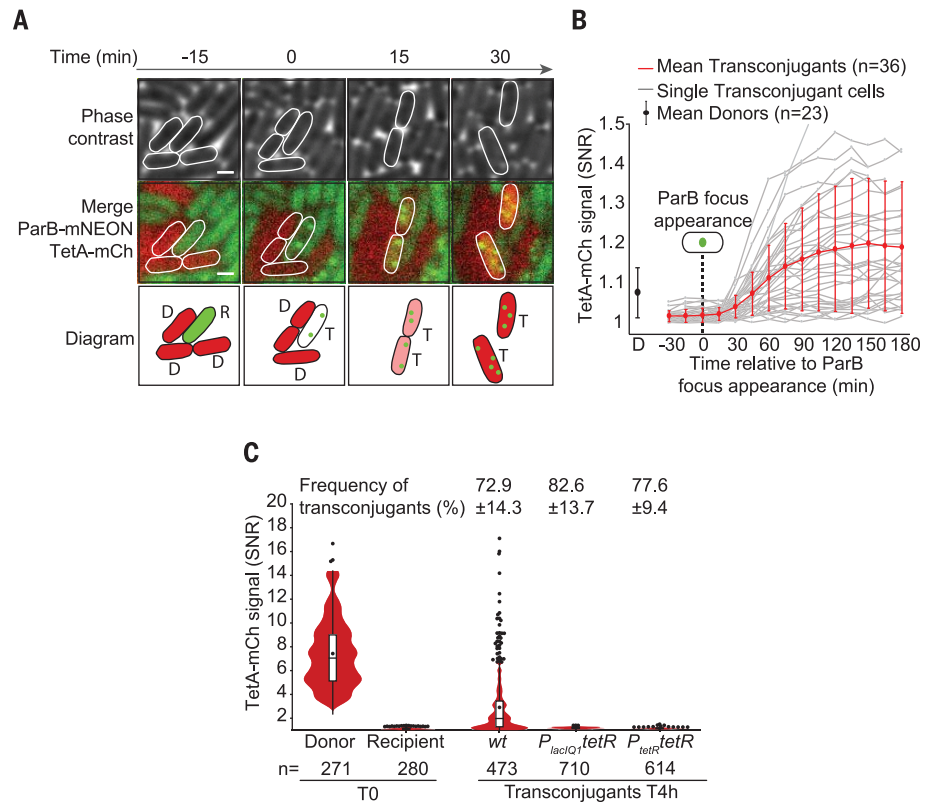


**Fig. 3. AcrAB-TolC is required for conjugation-mediated acquisition of resistance in the presence of tetracycline that inhibits protein synthesis.** (**A**) Frequency of Tc-resistant trans-conjugants through F-Tn10 transfer from WT donor to recipient cells in which AcrAB-TolC activity is compromised by ΔacrA, ΔacrB, or ΔtolC deletion. Donor and recipient CFU/ml in the conjugation mix are presented in fig. S10. (**B**) Violin plots showing TetA-mCh production at the single-cell level 8 hours after F-Tn10tetA-mCh plasmid transfer from WT donor to WT, ΔacrAB, ΔtolC, and ΔacrABΔtolC recipients, in the absence (left panel) or in the presence (right panel) of Tc. Same representation as in Fig. 1C. The number of cells analyzed (*n*) for one representative experiment is shown. Frequency of transconjugants and standard deviations are calculated from three independent experiments. (**C**) Quantification of Tc-induced ribosome-stalling in WT and in AcrAB-TolC mutant strains using pDualRep2 reporter plasmid. Histograms show the average fold-increase in Katushka2 fluorescence of the indicated strain treated with Tc. Standard deviation are calculated from at least three independent estimates. *P*-value significance is indicated by ns (>0.05, nonsignificant); *$P$ = 0.01 to 0.05 (significant); **$P$ = 0.001 to 0.01 (very significant); ***$P$ < 0.001 (extremely significant). Cropped images below the histogram show the induction of Katushka2 fluorescence at the periphery of the growth inhibition zone surrounding Tc-susceptibility disks.
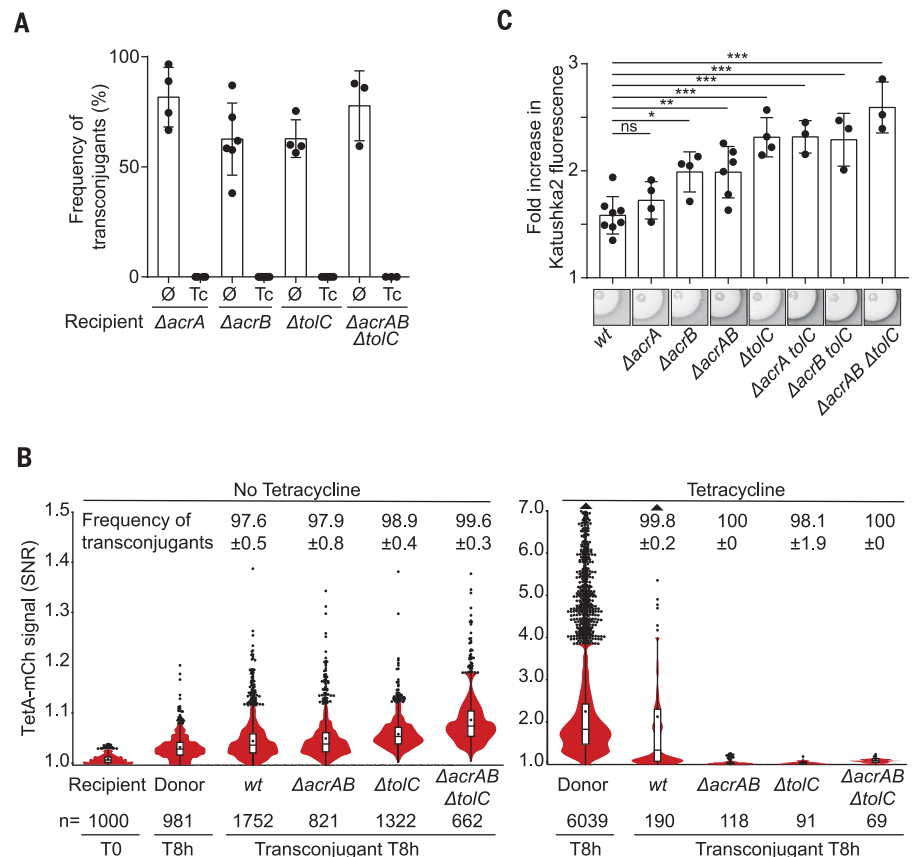
to Tc reduced but did not block the production of *sf*GFP. We conclude that protein synthesis is only partially inhibited by Tc in sensitive recipient cells. Continuing protein synthesis in the presence of Tc allows cells to produce TetA proteins to initiate Tc efflux, thus facilitating further synthesis of TetA and efflux activity. This positive feedback cycle gradually leads to effective Tc efflux and eventually restores protein synthesis.

Protein production levels observed after the acquisition of the Tc-resistance plasmid appear to be a product of the rate of entry of Tc molecules into the recipient cells and Tc-efflux activity mediated by TetA proteins that are accumulating in the cell. To subtract the contribution of TetA-mediated efflux, we quantified mCh production after transfer of the F plasmid carrying the deletion of *tetA* gene (F-Tn*10∆tetA::mCh*) in the presence of tetracycline. Surprisingly, plasmid acquisition was still followed by mCh production (fig. S5B), showing that synthesis of plasmid-encoded proteins in the presence of Tc occurs independently of TetA activity.

*E. coli* encodes an AcrAB-TolC multidrug efflux pump, which transports a range of xenobiotics from cell compartment to the extracellular medium and is responsible for a degree of intrinsic resistance to subinhibitory concentrations of a range of antibiotics (*25–29*) (fig. S6). To test whether the activity of this efflux pump helps to protect protein synthesis, and specifically TetA expression, we deleted *acrA*, *acrB*, or *tolC* genes. Mutant recipient cells failed to acquire resistance in the presence of tetracycline (Fig. 3A).

We excluded the possibility that the AcrAB-TolC mutant recipients were killed by Tc treatment before acquiring the plasmid by showing that transient exposure (up to 8 hours) to Tc, which is a bacteriostatic drug, does not affect the survival of single-, double-, or triple-mutant strains measured by plating assays (fig. S7A). We also showed that AcrAB-TolC mutant strains that carry the F-Tn*10* plasmid before Tc exposure showed normal resistance to Tc (fig. S7B), confirming that the AcrAB-TolC complex is not required for TetA-mediated resistance per se.

We used single-cell microscopy to evaluate TetA production after transfer of the F-Tn*10tetA-mCh* plasmid into AcrAB-TolC mutant recipient strains (Fig. 3B). Cells were analyzed 8 hours after conjugation, which allowed for high levels of TetA expression and unambiguous analysis. We observed that ∆*acrB*, ∆*tolC*, and ∆*acrB∆tolC* recipient strains can acquire the plasmid whether or not tetracycline is present. However, in the presence of tetracycline, plasmid acquisition is not followed by the production of TetA protein, and the transconjugant cells do not develop Tc resistance (Fig. 3B). Thus, AcrAB-TolC is essential for TetA production after plasmid acquisition when Tc is present.

In the presence of a growth-inhibiting concentration of Tc, AcrAB-TolC still performs efflux as revealed by Tc accumulation in ∆*acrA*, ∆*acrB*, and ∆*tolC* mutants compared with WT cells (fig. S7C). We tested if this low level of AcrAB-
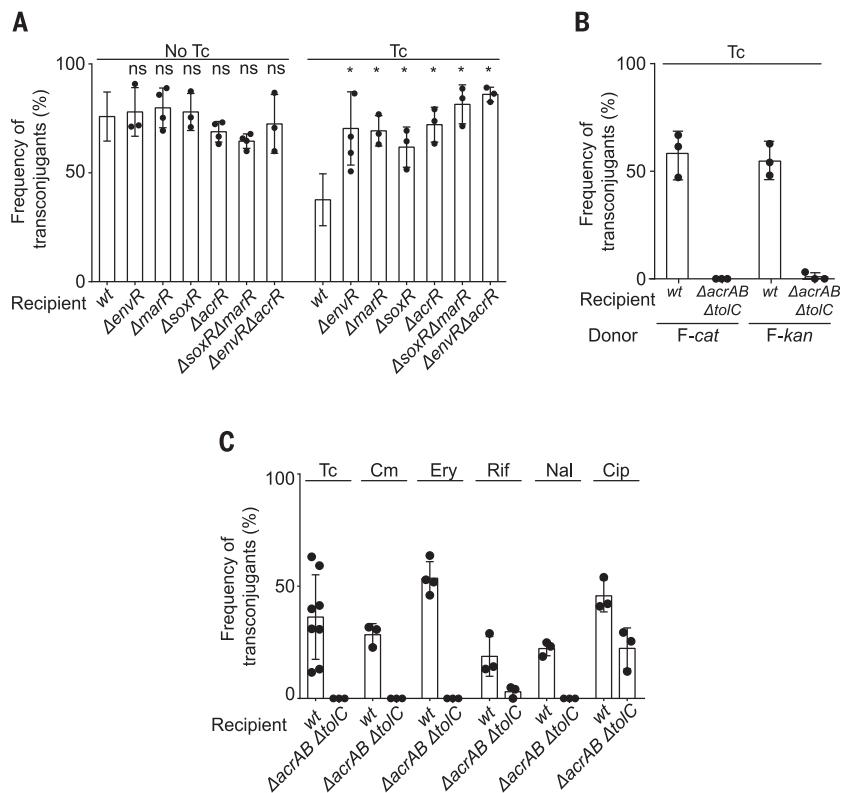


**Fig. 4. AcrAB-TolC regulation and activity influence drug-resistance acquisition.** (**A**) Frequency of Tc-resistant transconjugants through transfer of F-Tn*10* plasmid from WT donor into ∆*envR*, ∆*marR*, ∆*soxR*, and ∆*acrR* single- or double-deletion recipient strains, in the absence (No Tc) and in the presence of Tc. The values obtained for the WT recipient (Fig. 1A) were reported to facilitate the comparison. *P*-value significance from Mann-Whitney statistical test are indicated by ns (>0.05, nonsignificant) and *$P$ ≤ 0.008 (significant). (**B**) Frequency of Cm- and Kn-resistant transconjugants after the conjugation from a donor containing either the F plasmid carrying the *cat* gene (Cm resistance) or the *kan* gene (Kn resistance), in the presence of Tc. (**C**) Frequency of Tc-resistant transconjugants through transfer of the F-Tn*10* plasmid from a donor strain that is resistant to the tested antibiotic, toward a WT or ∆*acrAB∆tolC* recipient strain, in the presence of Tc, Cm, erythromycin (Ery), rifampicin (Rif), nalidixic acid (Nal), and ciprofloxacin (Cip). Donor and recipient CFU/ml in the conjugation mix corresponding to panels (A), (B), and (C) are presented in fig. S10.

TolC basal efflux activity, which is not sufficient to sustain cell growth, nonetheless allows some degree of protein synthesis to persist. We quantified the inhibitory effect of Tc on protein synthesis in WT and AcrAB-TolC mutant strains, using two independent assays. First, we used a reporter system specifically developed to quantify antibiotic-mediated ribosome stalling (*30, 31*) (Fig. 3C and supplementary materials). Results revealed that Tc-induced ribosome stalling activity occurred stepwise with sequential deletion of *acrA*, *acrB*, and *tolC*, with the maximal effect observed for the complete ∆*acrAB∆tolC* mutant. Second, we performed shotgun proteomic analysis after isobaric labeling of total proteins (*32*) in the WT, ∆*acrA*, ∆*acrB*, and ∆*tolC* strains before and after Tc treatment (fig. S8, data S1, and supplementary materials). We found that Tc treatment reduces the relative abundance of 28.5% of the detected proteins in WT cells. This percentage increases to 33.9, 41.8, and 47% in ∆*acrA*, ∆*acrB*, and ∆*tolC* mutants, respectively, corroborating

that the AcrAB-TolC complex facilitates protein synthesis in the presence of Tc.

AcrAB-TolC is tightly controlled by numerous transcriptional regulators, including the global repressors SoxR and MarR and the local repressors AcrR and EnvR (AcrS) (*27*). ∆*acrR*, ∆*envR*, ∆*marR*, and ∆*soxR* mutants exhibit enhanced resistance to subinhibitory concentrations of antibiotics (fig. S9A) and overproduction of the chromosomally encoded AcrB-GFP protein (*28*) (fig. S9B). In the absence of tetracycline, plasmid conjugation into these mutants resulted in Tc-resistance acquisition with the same efficiency as the WT recipient (Fig. 4A). However, in the presence of tetracycline, all four mutants showed increased ability to acquire Tc resistance. This result indicates that cells that have evolved regulatory mutations could acquire plasmid-mediated resistance more frequently than a WT strain.

AcrAB-TolC is essential for the acquisition of Tc resistance by horizontal gene transfer, presumably by reducing levels of Tc in the cell

enough to ensure that the synthesis of TetA resistance from the newly acquired plasmids can proceed. A similar biological mechanism could apply to the acquisition of other resistances by conjugation. In the presence of Tc, we also found that AcrAB-TolC is critical for the acquisition of chloramphenicol (Cm) and kanamycin (Kn) resistance, revealing its importance for the expression of the *cat* gene (encoding the chloramphenicol acetyltransferase) or the *kan* gene (encoding the aminoglycoside phosphotransferase from Tn*5*) carried by the F plasmid, respectively (Fig. 4B).

Finally, we tested the importance of AcrAB-TolC for the acquisition of Tc resistance in the presence of other drugs that are substrates of AcrAB-TolC. These experiments revealed that AcrAB-TolC is essential for the acquisition of Tc resistance in the presence of chloramphenicol and erythromycin (a macrolide), which both inhibit translation, and nalidixic acid, a quinolone that inhibits topoisomerases (Fig. 4C). AcrB-TolC is also important for the acquisition of resistance in the presence of rifampicin, which inhibits transcription, and ciprofloxacin, a fluoroquinolone that inhibits DNA gyrase (Fig. 4C). However, acquisition of resistance by AcrAB-TolC mutant recipients was still observed in the presence of the aminoglycoside translation inhibitor Kn, which also has a bactericidal effect (fig. S10, F and G, and supplementary materials). These results are consistent with the view that AcrAB-TolC efflux activity alleviates the inhibitory effect of drugs on the reactions that are required for resistance establishment after plasmid transfer, including conversion of plasmid ssDNA into dsDNA, transcription of the resistance gene into mRNA, and protein synthesis.

Our study reveals the key role of a multidrug efflux complex in preserving the acquisition of drug-specific resistance by horizontal gene transfer in the presence of bacterial inhibitors (fig. S11). The conservation of multidrug efflux pumps in virtually all bacterial genomes, combined with the large number of broad-host-range conjugative elements carrying multiple resistance determinants, raises the possibility that this mechanism plays a major role in the dissemination of drug resistance within bacterial communities. Given that possibility, antibiotic treatments that fail to prevent resistance transfer while exerting selection would increase the occurrence of resistance plasmids among diversified bacterial species.

## REFERENCES AND NOTES

1. M. N. Alekshun, S. B. Levy, *Cell* **128**, 1037–1050 (2007).
2. D. Mazel, J. Davies, *Cell. Mol. Life Sci.* **56**, 742–754 (1999).
3. M. Barlow, *Methods Mol. Biol.* **532**, 397–411 (2009).
4. P. M. Hawkey, A. M. Jones, *J. Antimicrob. Chemother.* **64** (suppl. 1), i3–i10 (2009).
5. J. Lederberg, E. L. Tatum, *Nature* **158**, 558 (1946).
6. E. L. Tatum, J. Lederberg, *J. Bacteriol.* **53**, 673–684 (1947).
7. K. A. Ippen-Ihler, E. G. Minkley Jr., *Annu. Rev. Genet.* **20**, 593–624 (1986).
8. F. de la Cruz, L. S. Frost, R. J. Meyer, E. L. Zechner, *FEMS Microbiol. Rev.* **34**, 18–40 (2010).
9. A. Ilangovan, S. Connery, G. Waksman, *Trends Microbiol.* **23**, 301–310 (2015).
10. H. J. Nielsen, J. R. Ottesen, B. Youngren, S. J. Austin, F. G. Hansen, *Mol. Microbiol.* **62**, 331–338 (2006).
11. R. Reyes-Lamothe, C. Possoz, O. Danilova, D. J. Sherratt, *Cell* **133**, 90–102 (2008).
12. F. Jacob, E. L. Wollman, *Symp. Soc. Exp. Biol.* **12**, 75–92 (1958).
13. E. Balleza, J. M. Kim, P. Cluzel, *Nat. Methods* **15**, 47–51 (2018).
14. J.-D. Pédelacq, S. Cabantous, T. Tran, T. C. Terwilliger, G. S. Waldo, *Nat. Biotechnol.* **24**, 79–88 (2006).
15. M. P. Calos, J. H. Miller, *Mol. Gen. Genet.* **183**, 559–560 (1981).
16. F. Jacob, E. L. Wollman, *Ann. Inst. Pasteur* **91**, 486–510 (1956).
17. A. Babić, A. B. Lindner, M. Vulić, E. J. Stewart, M. Radman, *Science* **319**, 1533–1536 (2008).
18. K. P. Bertrand, K. Postle, L. V. Wray Jr., W. S. Reznikoff, *J. Bacteriol.* **158**, 910–919 (1984).
19. D. W. Daniels, K. P. Bertrand, *J. Mol. Biol.* **184**, 599–610 (1985).
20. T. S. B. Møller *et al.*, *BMC Microbiol.* **16**, 39 (2016).
21. K. Biliouris, P. Daoutidis, Y. N. Kaznessis, *BMC Syst. Biol.* **5**, 9 (2011).
22. D. Schultz, A. C. Palmer, R. Kishony, *Cell Syst.* **5**, 509–517.e3 (2017).
23. B. Eckert, C. F. Beck, *J. Bacteriol.* **171**, 3557–3559 (1989).
24. A. J. Lopatkin *et al.*, *Nat. Microbiol.* **1**, 16044 (2016).
25. N. Tal, S. Schuldiner, *Proc. Natl. Acad. Sci. U.S.A.* **106**, 9051–9056 (2009).
26. D. Du *et al.*, *Nature* **509**, 512–515 (2014).
27. X.-Z. Li, P. Plésiat, H. Nikaido, *Clin. Microbiol. Rev.* **28**, 337–418 (2015).
28. T. Bergmiller *et al.*, *Science* **356**, 311–315 (2017).
29. M. C. Sulavik *et al.*, *Antimicrob. Agents Chemother.* **45**, 1126–1136 (2001).
30. I. A. Osterman *et al.*, *Antimicrob. Agents Chemother.* **56**, 1774–1783 (2012).
31. I. A. Osterman *et al.*, *Antimicrob. Agents Chemother.* **60**, 7481–7489 (2016).
32. N. Rauniyar, J. R. Yates 3rd, *J. Proteome Res.* **13**, 5293–5309 (2014).
33. A. Ducret, E. M. Quardokus, Y. V. Brun, *Nat. Microbiol.* **1**, 16077 (2016).
34. J. A. Vizcaíno *et al.*, *Nucleic Acids Res.* **44**, D447–D456 (2016).
35. F. Delolme, C. Lesterlin, Real-time visualization of drug resistance acquisition by horizontal gene transfer reveals a new role for AcrAB-TolC multidrug efflux pump, ProteomeXchange (2019); https://doi.org/10.6019/PXD011286.

## SUPPLEMENTARY MATERIALS

science.sciencemag.org/content/364/6442/778/suppl/DC1
Materials and Methods
Supplementary Text
Figs. S1 to S11
Tables S1 to S3
References (*36–41*)
Movies S1 to S7
Data S1

5 October 2018; accepted 15 April 2019
10.1126/science.aav6390

# Science

## Role of AcrAB-TolC multidrug efflux pump in drug-resistance acquisition by plasmid transfer

Sophie Nolivos, Julien Cayron, Annick Dedieu, Adeline Page, Frederic Delolme and Christian Lesterlin

### A race against time
Clinically relevant antimicrobial resistance is largely spread via plasmids that disperse among bacteria during conjugation. How quickly can a resistance gene be expressed after transfer? In susceptible bacterial cells, tetracycline should inhibit protein synthesis, including from the plasmid-transferred resistance gene *tetA*. Unexpectedly, Nolivos *et al.* found that TetA can be expressed despite the presence of tetracycline (see the Perspective by Povolo and Ackermann). Immediately after plasmid transfer into a cell, TetA synthesis starts because its repressor is slow to be expressed. In addition, the ubiquitous xenobiotic efflux pump AcrAB-TolC buys time for TetA translation by keeping tetracycline concentration below toxic levels.
*Science*, this issue p. 778; see also p. 737

| | |
|---|---|
| **ARTICLE TOOLS** | http://science.sciencemag.org/content/364/6442/778 |
| **SUPPLEMENTARY MATERIALS** | http://science.sciencemag.org/content/suppl/2019/05/22/364.6442.778.DC1 |
| **RELATED CONTENT** | http://science.sciencemag.org/content/sci/364/6442/737.full<br>http://stm.sciencemag.org/content/scitransmed/11/488/eaau9748.full<br>http://stm.sciencemag.org/content/scitransmed/9/410/eaal3693.full<br>http://stm.sciencemag.org/content/scitransmed/8/327/327ra25.full<br>http://stm.sciencemag.org/content/scitransmed/7/297/297ra114.full |
| **REFERENCES** | This article cites 40 articles, 15 of which you can access for free<br>http://science.sciencemag.org/content/364/6442/778#BIBL |
| **PERMISSIONS** | http://www.sciencemag.org/help/reprints-and-permissions |